

Cite this: *Nanoscale Adv.*, 2024, 6,  
3961

# Ni<sup>II</sup>-containing L-glutamic acid cross-linked chitosan anchored on Fe<sub>3</sub>O<sub>4</sub>/f-MWCNT: a sustainable catalyst for the green reduction and one-pot two-step reductive Schotten–Baumann-type acetylation of nitroarenes†

Hossein Mousavi, \* Behzad Zeynizadeh  and Morteza Hasanpour Galehban

In this research, new and eye-catching catalytic applications of the nickel<sup>II</sup> (Ni<sup>II</sup>) nanoparticles (NPs)-containing L-glutamic acid cross-linked chitosan anchored on magnetic carboxylic acid-functionalized multi-walled carbon nanotube (Fe<sub>3</sub>O<sub>4</sub>/f-MWCNT-CS-Glu/Ni<sup>II</sup>) system, which was characterized by Fourier transform infrared (FT-IR), powder X-ray diffraction (PXRD), scanning electron microscopy (SEM), transmission electron microscopy (TEM), SEM-based energy-dispersive X-ray (EDX) and elemental mapping, inductively coupled plasma-optical emission spectrometry (ICP-OES), thermogravimetric analysis (TGA), differential thermal analysis (DTA), and vibrating sample magnetometry (VSM), have been introduced for the environmentally benign and efficient reduction and one-pot two-step reductive Schotten–Baumann-type acetylation of nitroarenes in water at 60 °C under an air atmosphere. It is worth noting that the Ni<sup>II</sup>-containing hybrid nanocatalyst, in the mentioned organic reactions, showed short reaction times, high yields of the desired products, acceptable turnover numbers (TONs) and turnover frequencies (TOFs), and also satisfactory magnetic recycling and reusability performance even after ten times of reuse. As another significant point, all the titled organic transformations have been carried out in water as an entirely favorable and green solvent for chemical reactions.

Received 26th February 2024  
Accepted 28th May 2024

DOI: 10.1039/d4na00160e

rsc.li/nanoscale-advances

## 1. Introduction

The reduction (or hydrogenation) and conversion of aromatic nitro compounds, some of which are very hazardous<sup>1</sup> due to their carcinogenicity, non-biodegradability, and high toxicity, are used in a wide range of industrial and academic applications, such as environmental and water remediation, fuels, petroleum refining, explosives, batteries, dyes and pigments, rubber, photographic chemicals, agrochemicals, and also medicinal chemistry.<sup>2</sup> It is worth noting that aryl amines and *N*-aryl acetamides, which are among the most straightforward and practical compounds resulting from the chemical transformation of nitroarenes, are abundant in pharmaceutical and biological structures (Fig. 1). For example, as shown in Fig. 1, the mentioned structures existed in the backbone of amprevir (human immunodeficiency virus 1 (HIV-1) protease inhibitor), bromfenac (non-steroidal anti-inflammatory drug (NSAID)), sparfloxacin (antibiotic), mocetinostat (histone deacetylase 1 (HDAC-1) inhibitor), nomifensine

(norepinephrine-dopamine reuptake (NDR) inhibitor), garsorasib (KRAS<sup>G12C</sup> inhibitor), acetaminophen (non-opioid analgesic and antipyretic), and trametinib (mitogen-activated protein kinase kinases 1 and 2 (MEK-1 and MEK-2) inhibitor). In 2023, a boronate-based oxidant-responsive derivative of acetaminophen with IUPAC name (4-((4-acetamidophenoxy)methyl)phenyl)-boronic acid (Fig. 1, compound **I**) was reported as a proinhibitor of myeloperoxidase (MPO).<sup>3</sup> On the other hand, 4-acetamidophenyl(*S*)-2-(4-isobutylphenyl)propanoate (Fig. 1, compound **II**) was reported as a potential anti-nociceptive compound.<sup>4</sup> In another research paper, which was published in 2023, a new paracetamol-containing scaffold with IUPAC name *N*-(4-((5-(((1-(4-fluorophenyl)-1*H*-1,2,3-triazol-4-yl)methyl)thio)-1,3,4-oxadiazol-2-yl)methoxy)phenyl)acetamide (Fig. 1, compound **III**) was reported as a cyclooxygenase-2 (COX-2) inhibitor.<sup>5</sup>

In the past two or three decades, heterogeneous catalytic approaches have been picked as the logical synthetic methods for converting nitroarenes to beneficial compounds such as aryl amines and *N*-aryl acetamides. To this purpose, the fabrication of environmentally benign and capable catalytic systems has a remarkable impact on the mentioned organic transformations from the green chemistry point of view. It should be noted that the green chemistry principles have greatly influenced the

Department of Organic Chemistry, Faculty of Chemistry, Urmia University, Urmia, Iran. E-mail: 1hossein.mousavi@gmail.com

† Electronic supplementary information (ESI) available. See DOI: <https://doi.org/10.1039/d4na00160e>



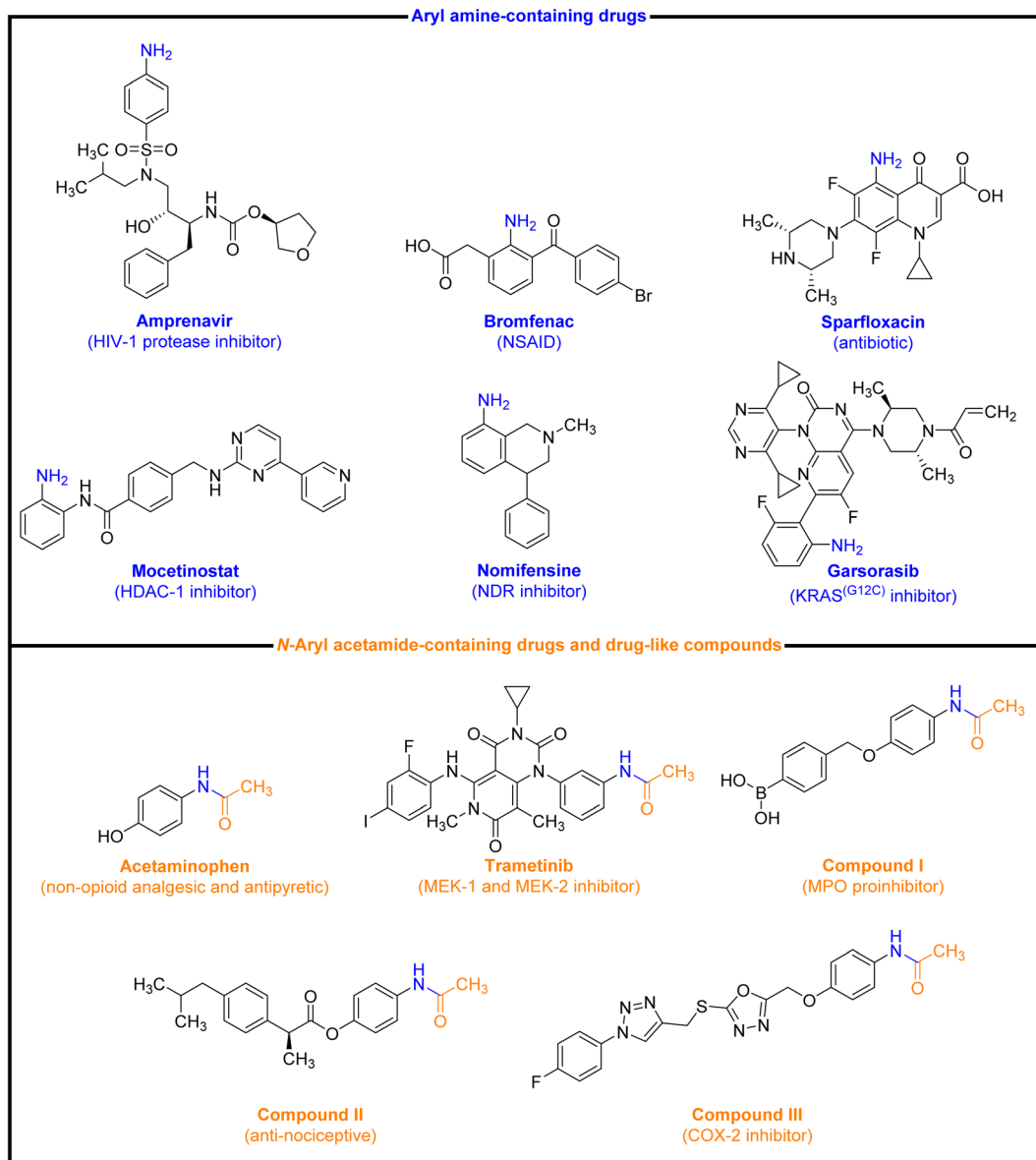


Fig. 1 Representative examples of drugs and drug-like compounds bearing aryl amine and *N*-aryl acetamide.

design of chemical reactions in recent years.<sup>6</sup> Based on green chemistry protocols, the design of magnetically recoverable nanocatalysts as brand-new heterogeneous catalytic systems is a suitable alternative for organic synthesis. In this regard, preparing and (or) designing an applicable and stable platform (and or supporter) for the catalyst scaffold construction are crucial. Chitosan (CS), as a *pseudo*-natural polysaccharide that is typically obtained from the alkaline *N*-deacetylation of chitin, is an outstanding biomacromolecule for developing new types of environmentally benign catalytic platforms and systems due to its unique, attractive, and natural properties such as biodegradability, biocompatibility, renewability, non-toxicity, affordability, simple recyclability, stability to air and moisture, thermal and chemical stability, high surface area, and insolubility in most of the organic solvents as well as aqueous reaction

mediums (except in acidic aqueous solutions), and many others.<sup>7</sup> Furthermore, the presence of diverse functional groups in the backbone of chitosan, including hydroxyl, amino, acetamido, and ether, along with chiral centers, makes chitosan an exceptional framework that can play many roles in catalysis science, especially the role of an excellent chelating and or coordinator agent for different metals, ions, and nanoparticles.<sup>7</sup> On the other hand, carbon nanomaterials are a prevalent choice as the best platform for developing catalytic systems since they can be manufactured in various physical structures and shapes with vital properties such as mechanical strength, pore dispersion, and thermal and chemical stability.<sup>8</sup> One of the well-known nanocarbons in science, especially in catalysis, is multi-walled carbon nanotubes (MWCNTs).<sup>9</sup>



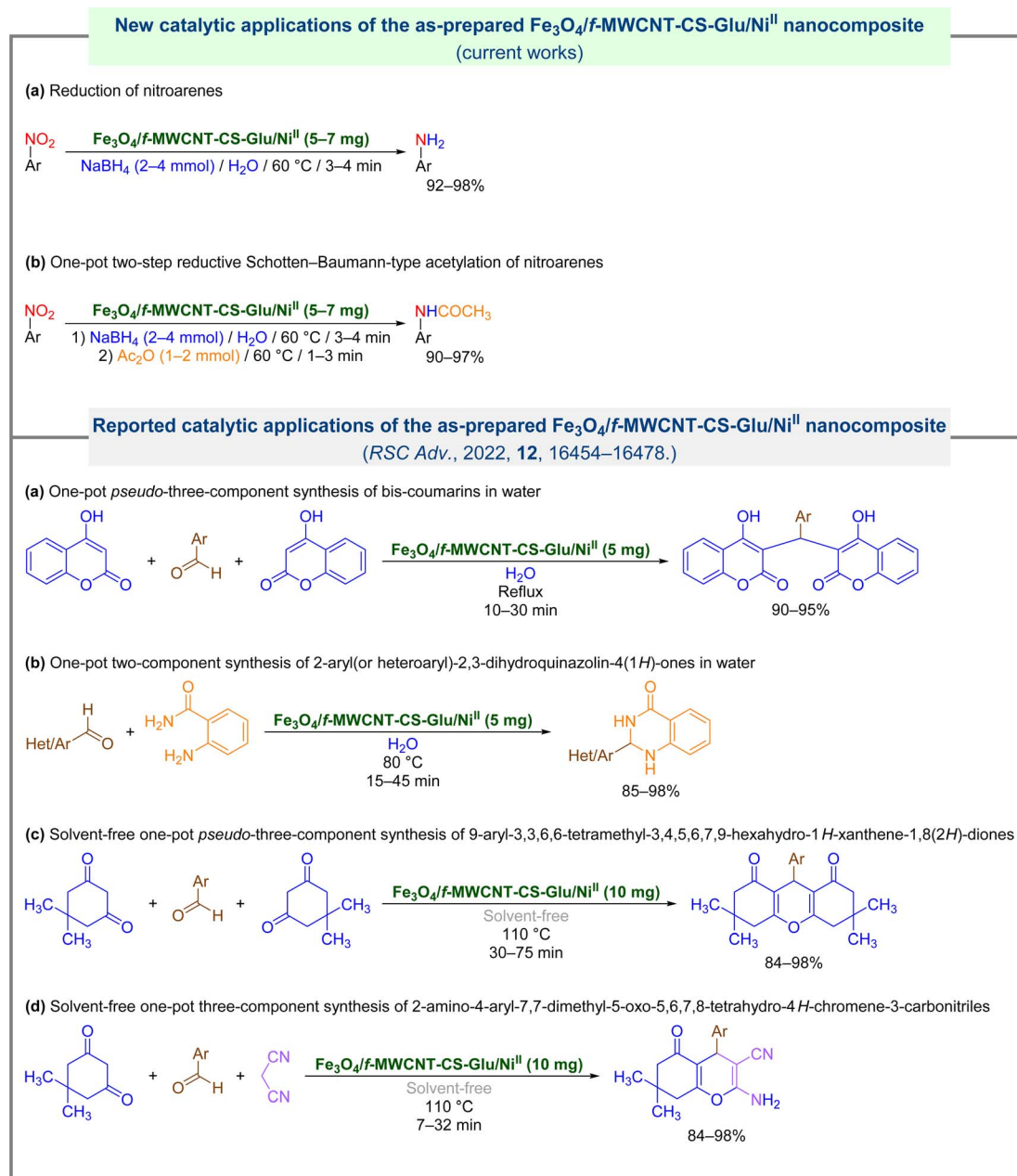


Fig. 2 Catalytic applications of the as-prepared Fe<sub>3</sub>O<sub>4</sub>/f-MWCNT-CS-Glu/Ni<sup>II</sup> nanocomposite.

Solvent is another significant factor from the green chemistry point of view. To this end, a list based on greenness has been introduced for known solvents in chemical reactions, and interestingly, ranked first in the mentioned list is water, and from most aspects, it is an ideal solvent for organic synthesis.<sup>19</sup>

In continuation of our research program on catalytic organic transformations,<sup>11,12</sup> and likewise, due to the importance of introducing new environmentally benign protocols to the conversion of nitroarenes to valuable organic compounds, herein we wish to report green and efficient strategies for the reduction and one-pot two-step reductive Schotten–Baumann-type acetylation of nitroarenes using the Fe<sub>3</sub>O<sub>4</sub>/f-MWCNT-CS-

Glu/Ni<sup>II</sup> nanocomposite as a powerful magnetically recoverable nanocatalytic system (Fig. 2).

## 2. Results and discussion

### 2.1. Preparation of the hybrid Fe<sub>3</sub>O<sub>4</sub>/f-MWCNT-CS-Glu/Ni<sup>II</sup> nanocomposite

We started our work with the preparation of the hybrid Fe<sub>3</sub>O<sub>4</sub>/f-MWCNT-CS-Glu/Ni<sup>II</sup> nanocomposite system according to our previous published paper in *RSC Advances* (Fig. 3).<sup>11</sup> Briefly, in step one, we used a sequential one-pot five-component strategy for the fabrication of L-glutamic acid cross-linked chitosan



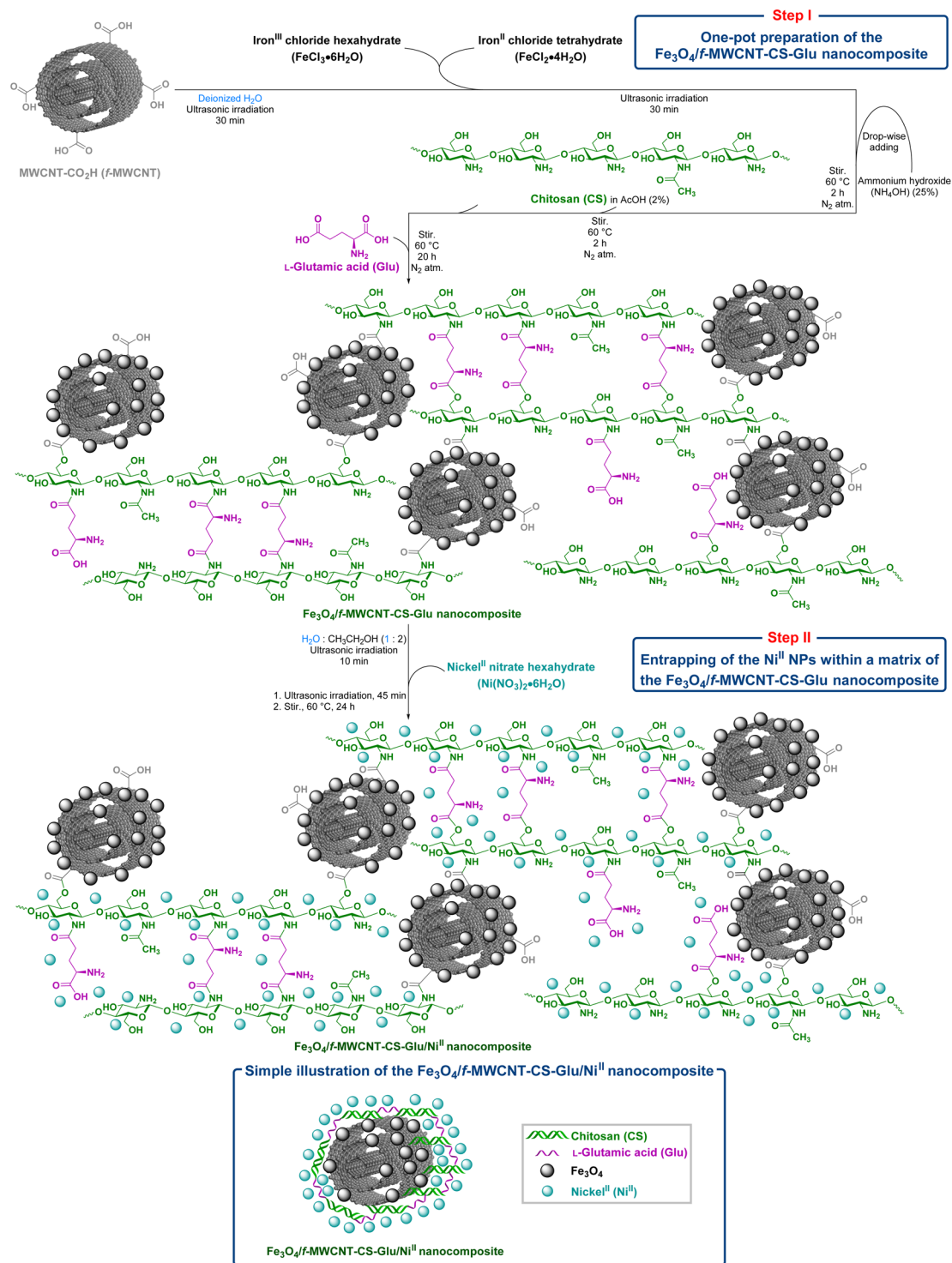


Fig. 3 Preparation pathway of the hybrid  $\text{Fe}_3\text{O}_4/\text{f-MWCNT-CS-Glu/Ni}^{\text{II}}$  nanocomposite.<sup>11</sup>

supported on magnetic carboxylic acid-functionalized multi-walled carbon nanotube ( $\text{Fe}_3\text{O}_4/\text{f-MWCNT-CS-Glu}$ ) (Fig. 3). After that, in the second step, by using nickel<sup>II</sup> nitrate hexahydrate ( $\text{Ni}(\text{NO}_3)_2 \cdot 6\text{H}_2\text{O}$ ) in the  $\text{H}_2\text{O} : \text{CH}_3\text{CH}_2\text{OH}$  (1 : 2) mixture under ultrasonic conditions, we immobilized the nickel<sup>II</sup> ( $\text{Ni}^{\text{II}}$ ) nanoparticles into the matrix of the prepared  $\text{Fe}_3\text{O}_4/\text{f-MWCNT-CS-Glu}$  nanocomposite to achieve the desired  $\text{Fe}_3\text{O}_4/\text{f-MWCNT-CS-Glu/Ni}^{\text{II}}$  nanocomposite (Fig. 3). It should be noted that the structure of the mentioned nanocomposite was previously fully characterized and examined by our group using Fourier transform infrared (FT-IR) (Fig. 4), powder X-ray diffraction (PXRD) (Fig. 5), scanning electron microscopy (SEM) (Fig. 6),

supported on magnetic carboxylic acid-functionalized multi-walled carbon nanotube ( $\text{Fe}_3\text{O}_4/\text{f-MWCNT-CS-Glu}$ ) (Fig. 3). After that, in the second step, by using nickel<sup>II</sup> nitrate hexahydrate ( $\text{Ni}(\text{NO}_3)_2 \cdot 6\text{H}_2\text{O}$ ) in the  $\text{H}_2\text{O} : \text{CH}_3\text{CH}_2\text{OH}$  (1 : 2) mixture under ultrasonic conditions, we immobilized the nickel<sup>II</sup> ( $\text{Ni}^{\text{II}}$ ) nanoparticles into the matrix of the prepared  $\text{Fe}_3\text{O}_4/\text{f-MWCNT-CS-Glu}$  nanocomposite to achieve the desired  $\text{Fe}_3\text{O}_4/\text{f-MWCNT-CS-Glu/Ni}^{\text{II}}$  nanocomposite (Fig. 3). It should be noted that the structure of the mentioned nanocomposite was previously fully characterized and examined by our group using Fourier transform infrared (FT-IR) (Fig. 4), powder X-ray diffraction (PXRD) (Fig. 5), scanning electron microscopy (SEM) (Fig. 6),



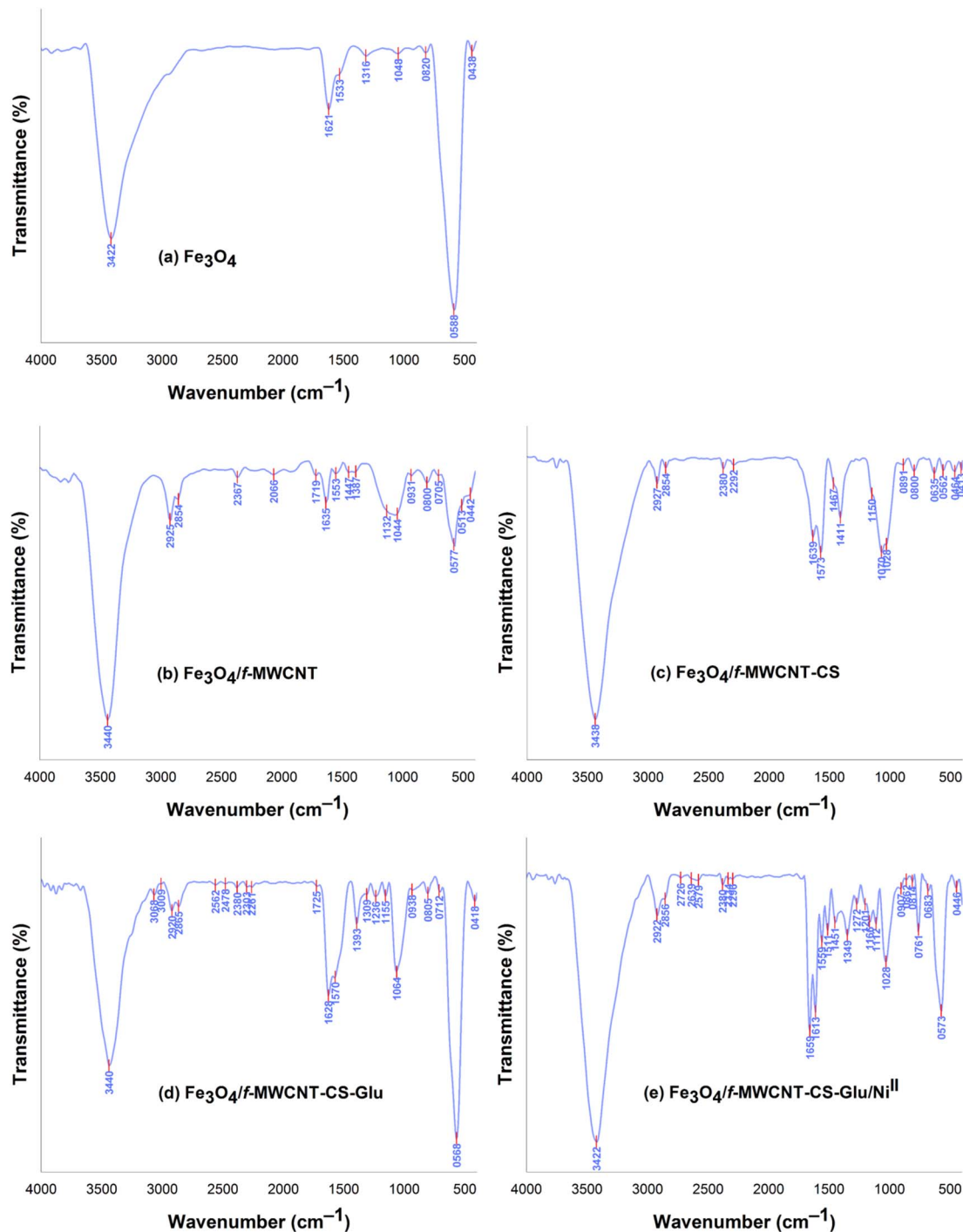


Fig. 4 FT-IR spectra of the  $\text{Fe}_3\text{O}_4$ ,  $\text{Fe}_3\text{O}_4/\text{f-MWCNT}$ ,  $\text{Fe}_3\text{O}_4/\text{f-MWCNT-CS}$ ,  $\text{Fe}_3\text{O}_4/\text{f-MWCNT-CS-Glu}$ , and  $\text{Fe}_3\text{O}_4/\text{f-MWCNT-CS-Glu/Ni}^{\text{II}}$  nanocomposites.<sup>11</sup>

transmission electron microscopy (TEM) (Fig. 7), SEM-based energy-dispersive X-ray spectroscopy (EDX) (Fig. 8) and elemental mapping (Fig. 9), inductively coupled plasma-optical emission spectrometry (ICP-OES), thermogravimetric analysis (TGA) (Fig. 10), differential thermal analysis (DTA) (Fig. 11), and vibrating sample magnetometry (VSM) (Fig. 12) analyses.<sup>11</sup>

## 2.2. Reduction of nitroarenes to the corresponding aryl amines

It is worth noting that the reduction (or hydrogenation) of nitroarenes is presently considered a benchmark reaction to test metal (or metal oxide)-containing nanocatalytic systems. In this regard, and after preparation of the hybrid  $\text{Fe}_3\text{O}_4/\text{f}$



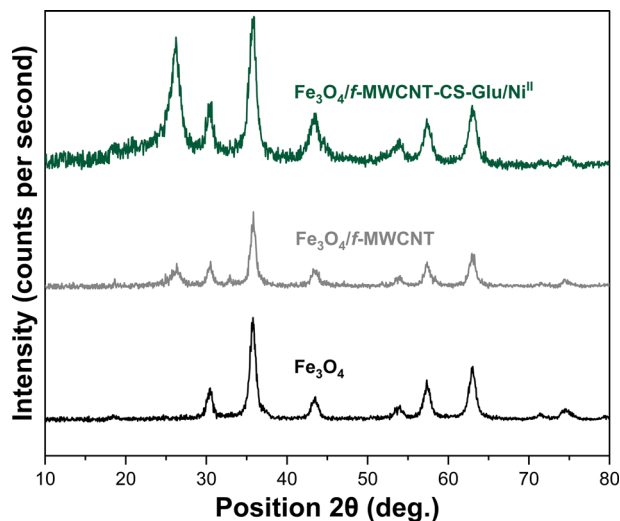


Fig. 5 XRD patterns of the  $\text{Fe}_3\text{O}_4$ ,  $\text{Fe}_3\text{O}_4/f\text{-MWCNT}$  and  $\text{Fe}_3\text{O}_4/f\text{-MWCNT-CS-Glu/Ni}^{\text{II}}$  nanocomposites.<sup>11</sup>

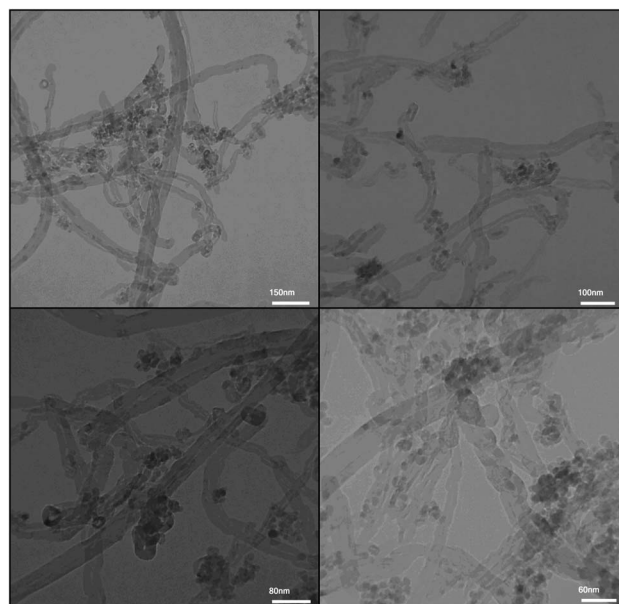


Fig. 7 TEM images of the as-prepared  $\text{Fe}_3\text{O}_4/f\text{-MWCNT-CS-Glu/Ni}^{\text{II}}$  nanocomposite.<sup>11</sup>

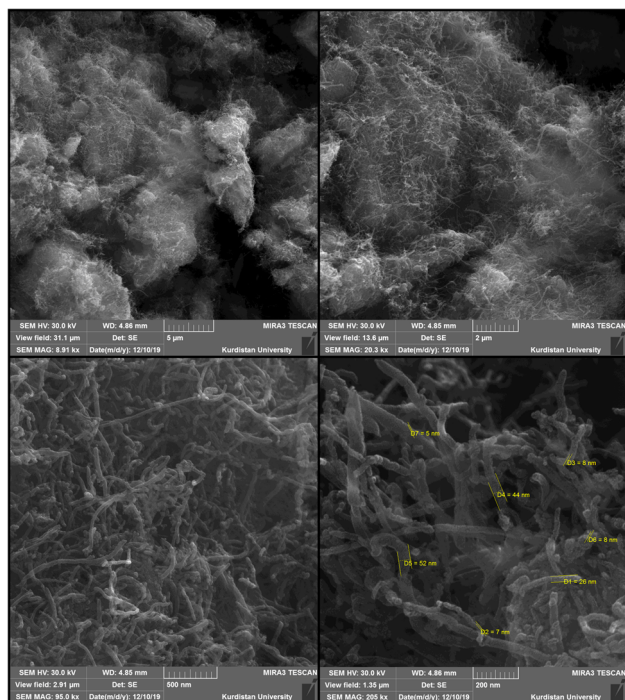


Fig. 6 SEM images of the as-prepared  $\text{Fe}_3\text{O}_4/f\text{-MWCNT-CS-Glu/Ni}^{\text{II}}$  nanocomposite.<sup>11</sup>

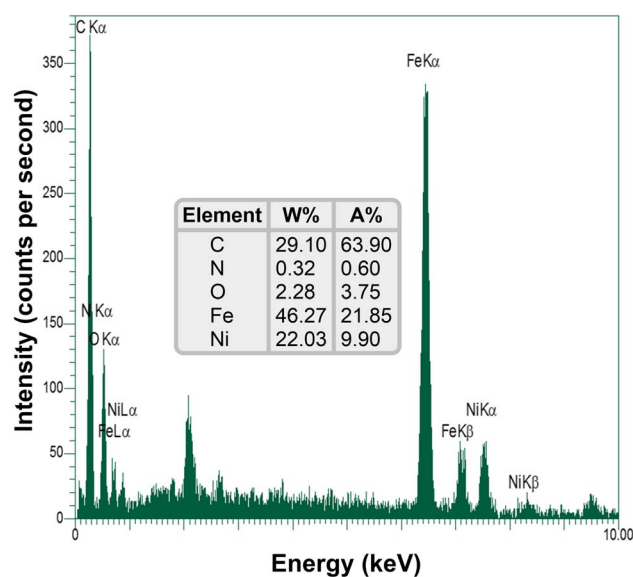


Fig. 8 SEM-based EDX diagram of the as-prepared  $\text{Fe}_3\text{O}_4/f\text{-MWCNT-CS-Glu/Ni}^{\text{II}}$  nanocomposite.<sup>11</sup>

MWCNT-CS-Glu/ $\text{Ni}^{\text{II}}$  nanocomposite, we started our work with reduction of nitrobenzene ( $\text{PhNO}_2$ ) to aniline ( $\text{PhNH}_2$ ) using 2 mmol of sodium borohydride ( $\text{NaBH}_4$ ) as a mild reducing agent in water at 60 °C in the presence of 5, 7, and 10 mg of the as-prepared  $\text{Fe}_3\text{O}_4/f\text{-MWCNT-CS-Glu/Ni}^{\text{II}}$  nanocatalyst (Table 1, entries 1–3), and it was found that increasing the amount of the nanocatalyst has no superior effect on the reaction and in all

cases the reaction was completed in 4 minutes. Notably, at room temperature, the mentioned reaction has a conversion rate of 50%, even after 60 minutes (Table 1, entry 4). Also, we screened the effect of various organic solvents, including  $\text{CH}_3\text{OH}$ ,  $\text{CH}_3\text{-CH}_2\text{OH}$ ,  $\text{CH}_3\text{CN}$ , *n*-hexane, and  $\text{CH}_2\text{Cl}_2$ , on the stated model reduction reaction in the presence of 5 mg of the mentioned  $\text{Ni}^{\text{II}}$ -containing nanocatalyst at 60 °C (Table 1, entries 5–9), and the results were utterly unsatisfactory. After the suitable reaction conditions have been established (Table 1, entry 1), the



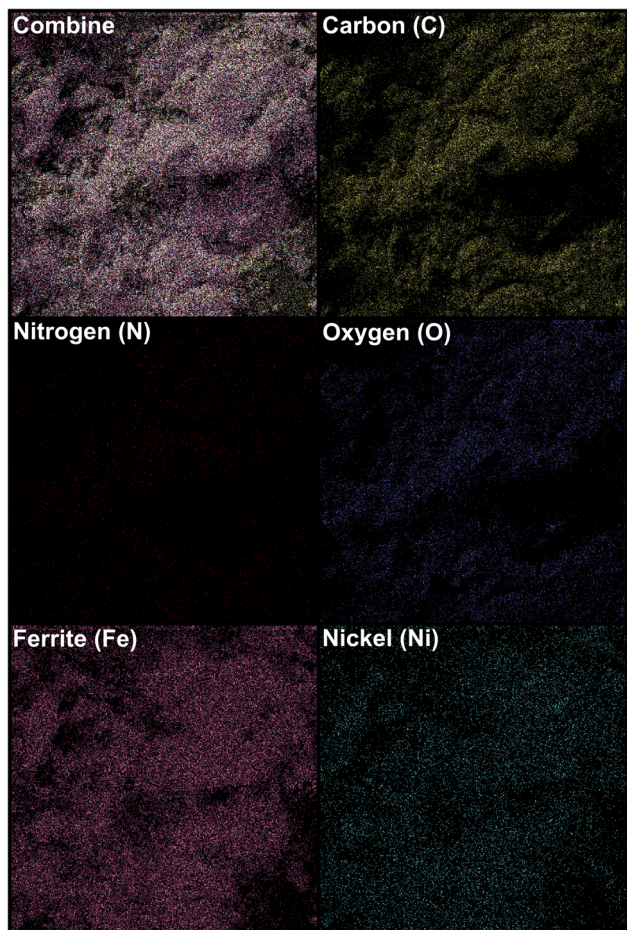


Fig. 9 SEM-based elemental mapping of the as-prepared  $\text{Fe}_3\text{O}_4/f\text{-MWCNT-CS-Glu/Ni}^{\text{II}}$  nanocomposite.<sup>11</sup>

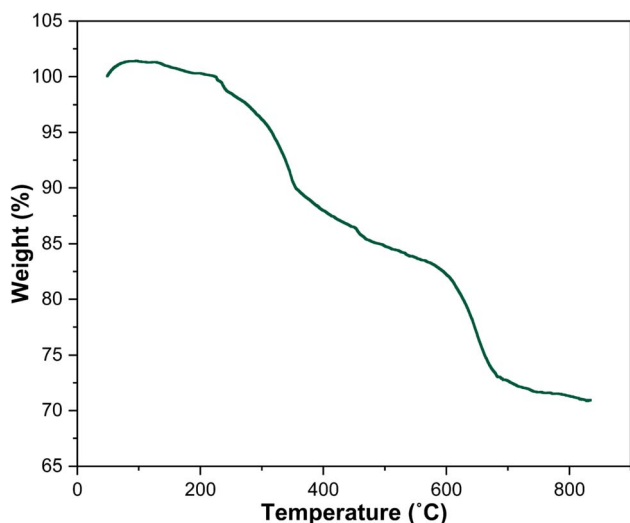


Fig. 10 TGA diagram of the as-prepared  $\text{Fe}_3\text{O}_4/f\text{-MWCNT-CS-Glu/Ni}^{\text{II}}$  nanocomposite.<sup>11</sup>

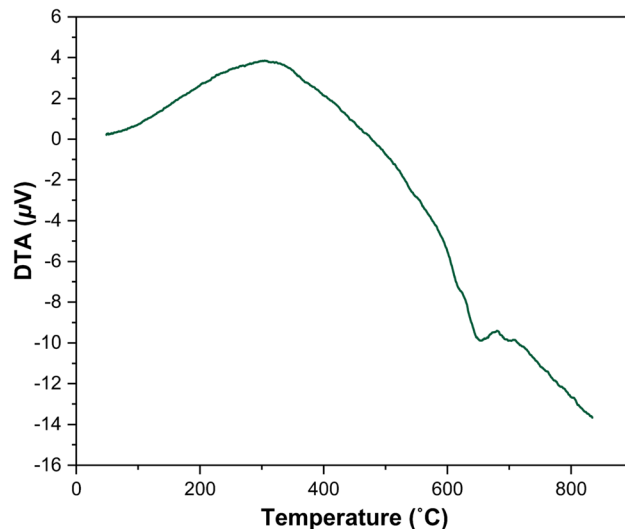


Fig. 11 DTA diagram of the as-prepared  $\text{Fe}_3\text{O}_4/f\text{-MWCNT-CS-Glu/Ni}^{\text{II}}$  nanocomposite.<sup>11</sup>

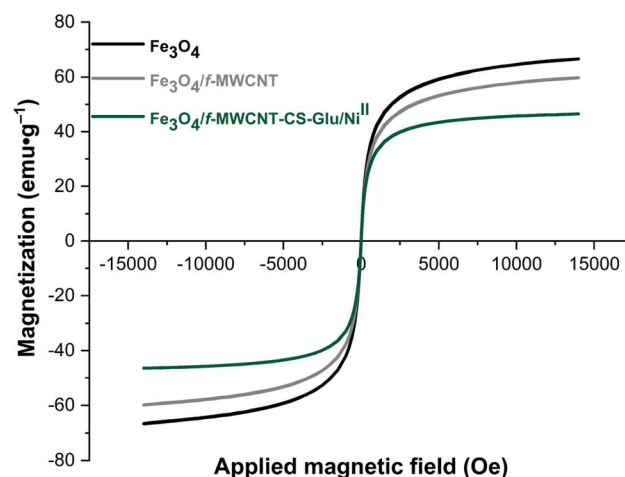


Fig. 12 VSM curves of the  $\text{Fe}_3\text{O}_4$ ,  $\text{Fe}_3\text{O}_4/f\text{-MWCNT}$ , and  $\text{Fe}_3\text{O}_4/f\text{-MWCNT-CS-Glu/Ni}^{\text{II}}$  nanocomposites.<sup>11</sup>

general efficiency of this protocol is delineated for the reduction of various nitroarenes (Table 2), and interestingly, all the reactions were completed rapidly with high yields. On the other hand, in these reactions, the turnover numbers (TONs) and turnover frequencies (TOFs) of the as-prepared  $\text{Fe}_3\text{O}_4/f\text{-MWCNT-CS-Glu/Ni}^{\text{II}}$  nanocatalyst were calculated and are listed in Table 2. Remarkably, the results of TONs and TOFs were acceptable and satisfactory.

### 2.3. One-pot two-step reductive Schotten-Baumann-type acetylation of nitroarenes to the corresponding aryl acetamides

As a matter of fact, the amide bond is one of the most common and precious functional elements that is abundantly present in



**Table 1** Optimization experiments for the reduction of PhNO<sub>2</sub> to PhNH<sub>2</sub> with NaBH<sub>4</sub> catalyzed by the hybrid Fe<sub>3</sub>O<sub>4</sub>/f-MWCNT-CS-Glu/Ni<sup>II</sup> nanocomposite

Entry	Catalyst (mg)	Solvent	Temperature conditions	Time (min)	Conversion (%)
1	5	H <sub>2</sub> O	60 °C	4	100
2	7	H <sub>2</sub> O	60 °C	4	100
3	10	H <sub>2</sub> O	60 °C	4	100
4	5	H <sub>2</sub> O	Room temperature	60	50
5	5	CH <sub>3</sub> OH	Reflux	120	35
6	5	CH <sub>3</sub> CH <sub>2</sub> OH	Reflux	120	35
7	5	CH <sub>3</sub> CN	Reflux	120	20
8	5	<i>n</i> -Hexane	Reflux	120	10
9	5	CH <sub>2</sub> Cl <sub>2</sub>	Reflux	120	0

the structure of drugs, agrochemicals, peptides, proteins, alkaloids, and many others.<sup>13</sup> In this context, introducing efficient, straightforward, and simple synthetic strategies for the construction of amide bonds is important. Also, acetylation of amines, especially aryl amines, is an effortless approach to the construction of an amide bond, and is extensively used in chemistry labs and the chemical industry.<sup>14</sup> It is imperative to bear in mind that nitroarenes are much cheaper than aryl amines in terms of price, and not only are one of the most important substrates for the preparation of aryl amines through a reduction process, but they are also toxic, and their transformation into other useful substances is valuable. Consequently, designing new protocols for the synthesis of aryl amides *via* straightforward one-pot reductive amidation (especially acetylation) of nitroarenes without isolation of the aryl amine intermediate is interesting. Furthermore, from the green chemistry point of view, one-pot reactions are recognized as a powerful tool in modern synthetic organic chemistry, which leads to a clear and tangible decrease in the consumption of reagents, auxiliaries, catalysts and or promoters, and solvents and consequently causes minimization of waste, energy, and time.<sup>15</sup> In this regard, and after obtaining the successful strategy for the reduction of nitroarenes, we decided to introduce a new

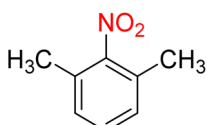
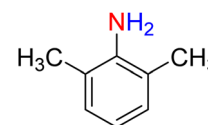
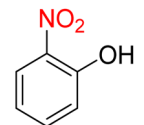
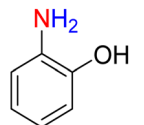
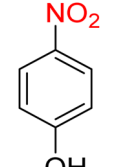
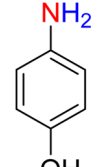
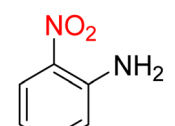
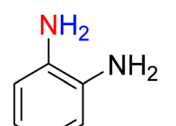
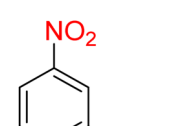
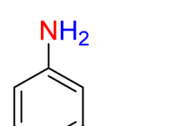
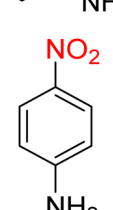
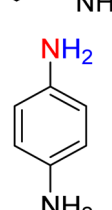
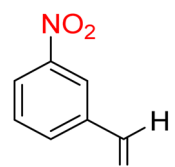
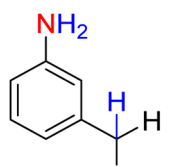
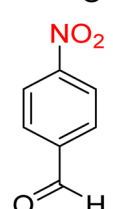
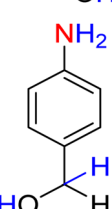
**Table 2** Reduction of nitroarenes to corresponding aryl amines using NaBH<sub>4</sub> catalyzed by the Fe<sub>3</sub>O<sub>4</sub>/f-MWCNT-CS-Glu/Ni<sup>II</sup> nanocomposite in water<sup>a</sup>

Entry	Substrate	Product	RMCR	Time (min)	Yield (%)	TON	TOF (min <sup>-1</sup> )
1			1 : 2 : 5	4	98	93.37587	23.34397
2			1 : 2 : 5	4	95	90.51742	22.62935
3			1 : 2 : 5	3	94	89.56461	29.85487
4			1 : 2 : 5	3	94	89.56461	29.85487
5			1 : 2 : 5	4	96	91.47024	22.86756





Table 2 (Contd.)

Entry	Substrate	Product	RMCR	Time (min)	Yield (%)	TON	TOF (min <sup>-1</sup> )
$\text{Ar}-\text{NO}_2 \xrightarrow[\text{NaBH}_4 (2-4 \text{ mmol}) / \text{H}_2\text{O} (3 \text{ mL}) / 60 \text{ }^\circ\text{C} / 3-4 \text{ min}]{\text{Fe}_3\text{O}_4/f\text{-MWCNT-CS-Glu/Ni}^{\text{II}} (5-7 \text{ mg})} \text{Ar}-\text{NH}_2$ 92–98%							
6			1 : 2 : 5	4	95	90.51742	22.62935
7			1 : 2 : 5	4	93	88.61179	22.15295
8			1 : 2 : 5	4	94	89.56461	29.85487
9			1 : 2 : 5	3	94	89.56461	29.85487
10			1 : 2 : 5	4	97	92.42305	23.10576
11			1 : 2 : 5	3	95	90.51742	30.17247
11			1 : 4 : 7	3	92	62.61355	20.87118
12			1 : 4 : 7	4	93	63.29414	15.82353

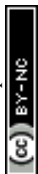


Table 2 (Contd.)

Entry	Substrate	Product	RMCR	Time (min)	Yield (%)	TON	TOF (min <sup>-1</sup> )
	$\text{Ar}-\text{NO}_2 \xrightarrow[\text{NaBH}_4 (2-4 \text{ mmol}) / \text{H}_2\text{O} (3 \text{ mL}) / 60^\circ\text{C} / 3-4 \text{ min}]{\text{Fe}_3\text{O}_4/f\text{-MWCNT-CS-Glu/Ni}^{\text{II}} (5-7 \text{ mg})} \text{Ar}-\text{NH}_2$ 92–98%						
13			1 : 4 : 7	4	95	64.65530	16.16382
14			1 : 4 : 7	3	96	65.33588	21.77863
15			1 : 4 : 7	4	92	62.61355	15.65339

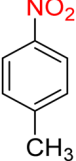
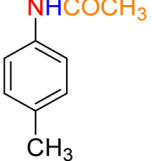
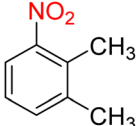

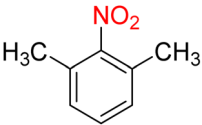

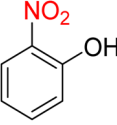
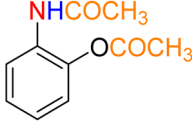
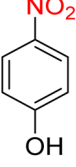
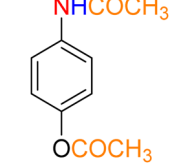
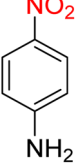

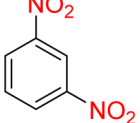
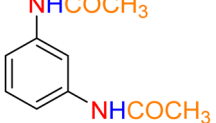
<sup>a</sup> RMCR (reaction main components ratio) = substrate (mmol) : NaBH<sub>4</sub> (mmol) : catalyst (mg). Yields refer to isolated pure products. TON (turnover number) = [(mol of the product formed)/(mol of the catalyst used)]. TOF (turnover frequency) = [(mol of the product formed)/(mol of the catalyst used) × (time)]. The TON and TOF values were calculated based on the existing amount of nickel (Ni) in the as-prepared nanocatalyst (in 5 mg of the hybrid nanocatalyst, 0.616 mg (or 0.010495217 mmol) of Ni exists).

Table 3 One-pot two-step reductive Schotten–Baumann-type acetylation of nitroarenes catalyzed by the Fe<sub>3</sub>O<sub>4</sub>/f-MWCNT-CS-Glu/Ni<sup>II</sup> nanocomposite in water<sup>a</sup>

Entry	Substrate	Product	Molar ratio	Time (min)	Yield (%)	TON	TOF (min <sup>-1</sup> )
	$\text{Ar}-\text{NO}_2 \xrightarrow[\text{2) Ac}_2\text{O} (1-2 \text{ mmol}) / 60^\circ\text{C} / 1-3 \text{ min}]{\text{NaBH}_4 (2-4 \text{ mmol}) / \text{H}_2\text{O} (3 \text{ mL}) / 60^\circ\text{C} / 3-4 \text{ min}} \text{Ar}-\text{NHCOCH}_3$ 90–97%						
1			1 : 2 : 5 : 1	5	97	92.42305	18.48461
2			1 : 2 : 5 : 1	5	94	89.56461	17.91292
3			1 : 2 : 5 : 1	4	93	88.61179	22.15295



Table 3 (Contd.)

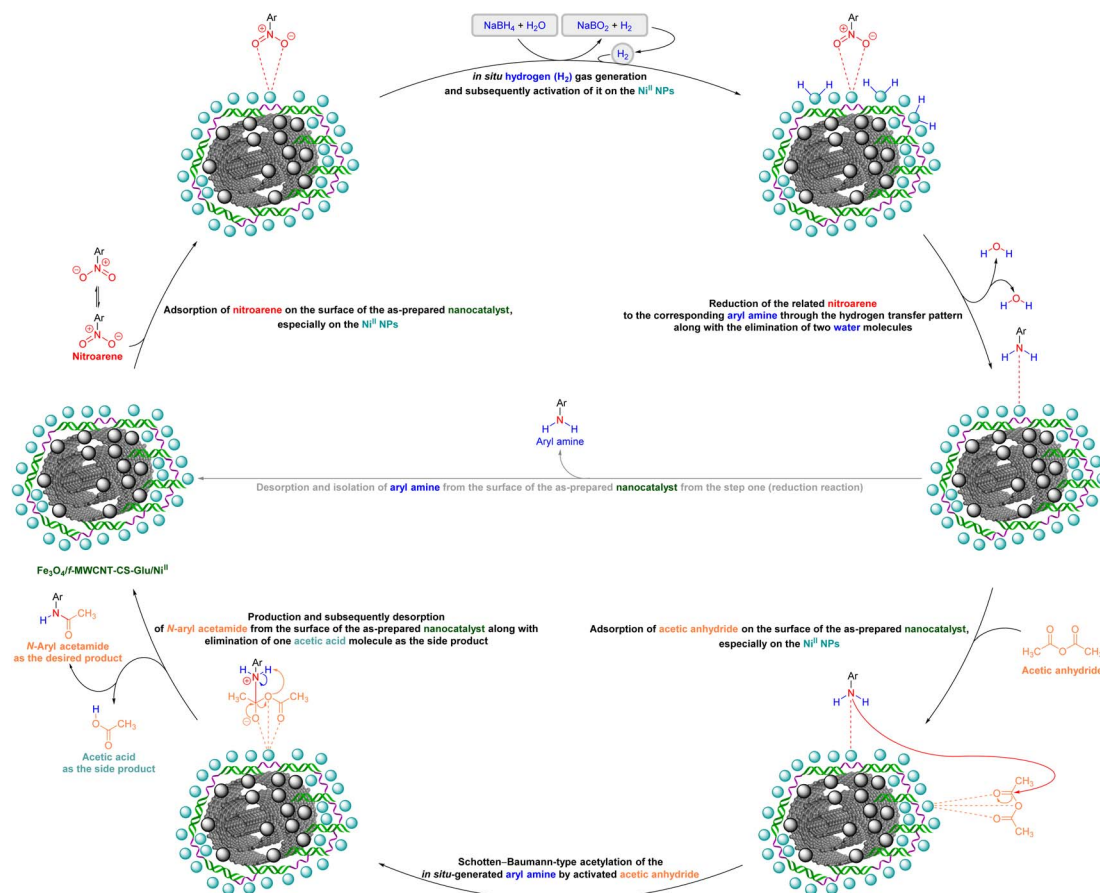
Entry	Substrate	Product	Molar ratio	Time (min)	Yield (%)	TON	TOF (min <sup>-1</sup> )
	$\text{Ar}-\text{NO}_2 \xrightarrow[\text{2) Ac}_2\text{O (1-2 mmol) / 60 }^\circ\text{C / 1-3 min}]{\text{Fe}_3\text{O}_4/\text{f-MWCNT-CS-Glu/Ni}^{\text{II}} \text{ (5-7 mg) / NaBH}_4 \text{ (2-4 mmol) / H}_2\text{O (3 mL) / 60 }^\circ\text{C / 3-4 min}} \text{Ar}-\text{NHCOCH}_3$ <p style="text-align: right;">90–97%</p>						
4			1 : 2 : 5 : 1	4	92	87.65898	21.91474
5			1 : 2 : 5 : 1	6	94	89.56461	14.92743
6			1 : 2 : 5 : 1	7	91	86.70616	12.38659
7			1 : 2 : 5 : 2	7	90	85.75335	12.25048
8			1 : 2 : 5 : 2	5	90	85.75335	17.15067
9			1 : 2 : 5 : 2	4	92	87.65898	21.91474
10			1 : 4 : 7 : 2	7	91	61.93297	8.84756

<sup>a</sup> RMCR (reaction main components ratio) = substrate (mmol) : NaBH<sub>4</sub> (mmol) : catalyst (mg) : Ac<sub>2</sub>O (mmol). Yields refer to isolated pure products. TON (turnover number) = [(mol of the product formed)/(mol of the catalyst used)]. TOF (turnover frequency) = [(mol of the product formed)/(mol of the catalyst used) × (time)]. The TON and TOF values were calculated based on the existing amount of nickel (Ni) in the as-prepared nanocatalyst (in 5 mg of the hybrid nanocatalyst, 0.616 mg (or 0.010495217 mmol) of Ni exists).

one-pot two-step reductive Schotten–Baumann-type acetylation approach for the efficient and green synthesis of *N*-aryl acetamides from aromatic nitro compounds. To this purpose, in the second step of the mentioned one-pot organic transformation (*viz.* Schotten–Baumann-type acetylation), we used 1 mmol of

acetic anhydride (Ac<sub>2</sub>O) as an acetylating agent under the same temperature conditions (60 °C). As shown in Table 3, we successfully prepared diverse *N*-aryl acetamide derivatives, and it was found that the acetylation step is faster than the reduction step. Notably, according to the amount of catalyst used, our





Scheme 1 Plausible and concise mechanism for the one-pot two-step reductive Schotten–Baumann-type acetylation of nitroarenes catalyzed by the  $\text{Fe}_3\text{O}_4/\text{f-MWCNT-CS-Glu}/\text{Ni}^{\text{II}}$  nanocomposite.

presented one-pot protocol has acceptable reaction times, yields, and TON and TOF values for the mentioned two-step organic transformation (Table 3). Furthermore, a plausible and concise mechanism for the current one-pot two-step reductive Schotten–Baumann-type acetylation reaction in the presence of the as-prepared  $\text{Ni}^{\text{II}}$ -containing hybrid nanocatalyst is depicted in Scheme 1.

#### 2.4. Recoverability, reusability, and hot filtration test experiments of the as-prepared $\text{Fe}_3\text{O}_4/\text{f-MWCNT-CS-Glu}/\text{Ni}^{\text{II}}$ nanocomposite

In the last stage of the present work, the recyclability and reusability of the as-prepared  $\text{Fe}_3\text{O}_4/\text{f-MWCNT-CS-Glu}/\text{Ni}^{\text{II}}$  nanocomposite and its hot filtration test have been evaluated. In this regard, it seems necessary to point out two points. First, in some cases, chitosan-based catalytic systems suffer from mechanical and thermal stability that modification of chitosan (CS) through an additional process (such as a cross-linking process) not only improves but also can lead to the decrease of metal leaching.<sup>16</sup> The thermal stability of the mentioned hybrid

catalytic system not only is unique for the current organic transformations, which were carried out at 60 °C, but also is excellent even for most chemical reactions because, as shown in the TGA diagram, the structure of this nanocomposite is completely stable up to 225 °C, and just a 1% weight loss was observed below 240 °C, which may be related to the solvent and moisture evaporations (Fig. 10). Second, the VSM analysis demonstrated that the saturation magnetization ( $M_s$ ) amount of the as-prepared  $\text{Fe}_3\text{O}_4/\text{f-MWCNT-CS-Glu}/\text{Ni}^{\text{II}}$  nanocatalyst was 19.743  $\text{emu g}^{-1}$  which is suitable for a high magnetic recycling and reusability performance (Fig. 12). The recyclability and reusability experiments of the as-prepared superparamagnetic  $\text{Ni}^{\text{II}}$ -containing nanocatalyst, which were carried out on the reduction of  $\text{PhNO}_2$  (1 mmol) to  $\text{PhNH}_2$  using  $\text{NaBH}_4$  (2 mmol) in the presence of the as-prepared  $\text{Fe}_3\text{O}_4/\text{f-MWCNT-CS-Glu}/\text{Ni}^{\text{II}}$  (5 mg) nanocatalyst in water at 60 °C as a model reaction, revealed satisfactory results even after ten runs (Fig. 13, section a). On the other hand, the hot filtration test was also performed for the further investigation upon leaching of the  $\text{Ni}^{\text{II}}$  NPs in the aforementioned model reaction, and it was found that separation of the whole of the  $\text{Fe}_3\text{O}_4/\text{f-MWCNT-CS-Glu}/\text{Ni}^{\text{II}}$



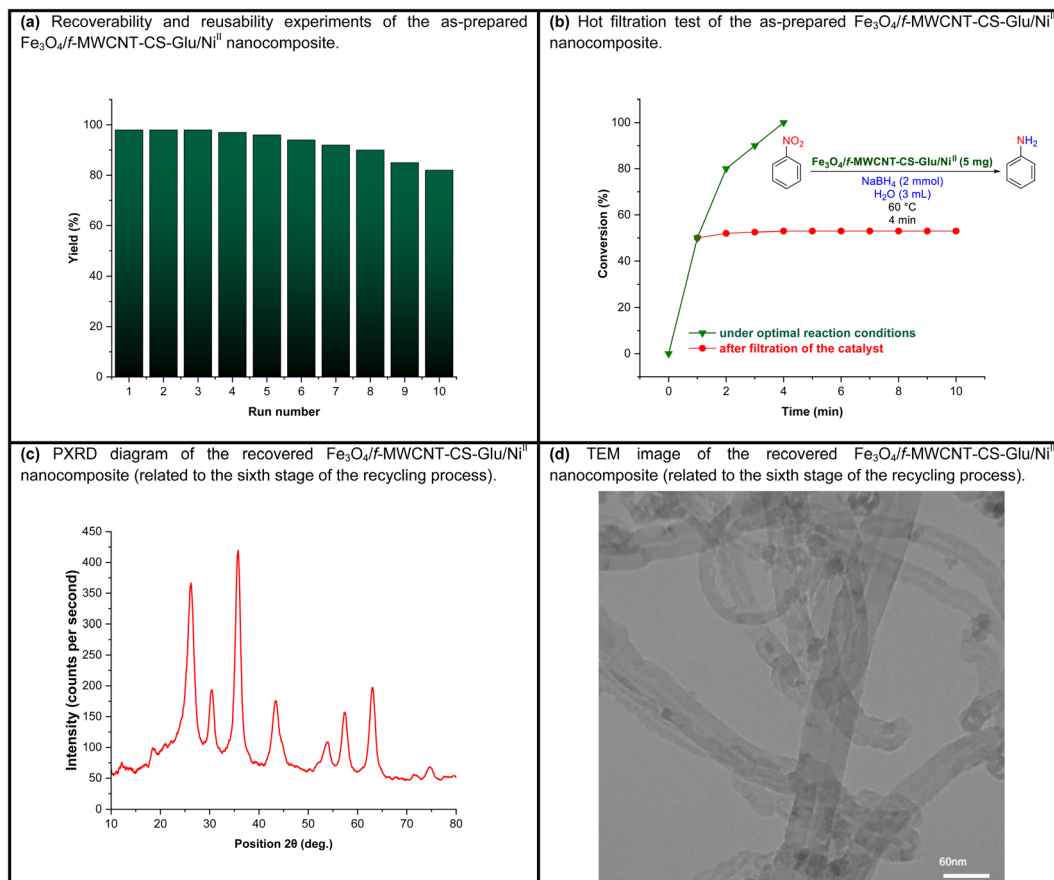


Fig. 13 Recoverability and reusability experiments (a) and hot filtration test (b) of the as-prepared  $\text{Fe}_3\text{O}_4/\text{f-MWCNT-CS-Glu/Ni}^{\text{II}}$  nanocatalyst, along with the PXRD pattern (c) and TEM image (d) of the recovered  $\text{Fe}_3\text{O}_4/\text{f-MWCNT-CS-Glu/Ni}^{\text{II}}$  nanocomposite.

nanocatalytic system from the mentioned reaction environment (when the conversion rate was 50%) caused no substantial improvement in the reaction process, which clearly confirmed satisfactory stability of the  $\text{Ni}^{\text{II}}$  NPs in the  $\text{Fe}_3\text{O}_4/\text{f-MWCNT-CS-Glu}$  matrix (Fig. 13, section b). Moreover, the PXRD pattern (Fig. 13, section c) and a TEM image (Fig. 13, section d) of the recovered  $\text{Fe}_3\text{O}_4/\text{f-MWCNT-CS-Glu/Ni}^{\text{II}}$  nanocomposite after the sixth recycling step have been demonstrated, which shows that the structure of the mentioned  $\text{Ni}^{\text{II}}$ -containing nanocomposite remained intact. Furthermore, the leaching test results obtained by ICP-OES measurements revealed that the amount of nickel (Ni) decreased from 12.3 w% to 11.2 w% after the sixth run.

### 2.5. A comparative study

To demonstrate the efficiency and capability of our new green synthetic protocols on the reduction and one-pot two-step reductive Schotten–Baumann-type acetylation of nitroarenes in the presence of the as-prepared hybrid  $\text{Fe}_3\text{O}_4/\text{f-MWCNT-CS-Glu/Ni}^{\text{II}}$  nanocomposite as an influential catalytic system in water, they have been compared with some of the previously reported procedures. As shown in Table 4, the obtained results clearly demonstrated that the current green synthetic strategies have

a suitable place in terms of efficiency and greenness compared to the previously published protocols.

## 3. Conclusions

In this paper, we successfully demonstrated that entrapping  $\text{Ni}^{\text{II}}$  nanoparticles within a matrix of *L*-glutamic acid cross-linked chitosan supported on magnetic carboxylic acid-functionalized multi-walled carbon nanotube causes a unique hybrid earth-abundant transition metal-containing nanocomposite ( $\text{Fe}_3\text{O}_4/\text{f-MWCNT-CS-Glu/Ni}^{\text{II}}$ ) as an effective and sustainable nanocatalytic system for the environmentally benign and efficient reduction and one-pot two-step reductive Schotten–Baumann-type acetylation of nitroarenes in water at  $60^\circ\text{C}$  under an air atmosphere. The salient features of the presented synthetic protocols are short reaction times, high yields of the desired products, acceptable TONs and TOFs, and satisfactory recyclability and reusability of the catalyst. Notably, research to find and develop new and green nanocatalytic systems containing various earth-abundant transition metals to achieve highly efficient protocols for the conversion of hazardous aromatic nitro compounds to corresponding aryl amines, aryl acetamides, and or other valuable organic compounds is currently underway in our research group.



**Table 4** Comparison of the catalytic activity of the as-prepared Fe<sub>3</sub>O<sub>4</sub>/f-MWCNT-CS-Glu/Ni<sup>II</sup> nanocomposite with literature samples reported on reduction and one-pot reductive acetylation of nitrobenzene

Part A				
Entry	Reaction conditions	Time	Yield	Ref.
A1	Fe <sub>3</sub> O <sub>4</sub> /f-MWCNT-CS-Glu/Ni <sup>II</sup> (5 mg); NaBH <sub>4</sub> (2 mmol); H <sub>2</sub> O; 60 °C	4 min	98%	<sup>a</sup>
A2	Fe <sub>3</sub> O <sub>4</sub> @SiO <sub>2</sub> @KCC-1@MPTMS@Cu <sup>II</sup> (10 mg); NaBH <sub>4</sub> (2 mmol); H <sub>2</sub> O; 60 °C	5 min	98%	12b
A3	(7 wt%) Pd/C (30 mg); NaBH <sub>4</sub> (2 mmol); H <sub>2</sub> O; reflux	7 min	93%	12c
A4	CuFe <sub>2</sub> O <sub>4</sub> (48 mg); NaBH <sub>4</sub> (2 mmol); H <sub>2</sub> O; reflux	50 min	95%	12h
A5	Ni <sub>2</sub> B@Cu <sub>2</sub> O (54 mg); NaBH <sub>4</sub> (2.5 mmol); wet-solvent-free grinding; r.t.	1 min	98%	12j
A6	Ni <sub>2</sub> B@CuCl <sub>2</sub> (52 mg); NaBH <sub>4</sub> (2.5 mmol); wet-solvent-free grinding; r.t.	2 min	98%	12j
A7	Fe <sub>2</sub> Se <sub>2</sub> CO <sub>9</sub> (3 mol%); NH <sub>2</sub> NH <sub>2</sub> ·H <sub>2</sub> O (2 mmol); H <sub>2</sub> O; 110 °C	15 min	89%	17
A8	Ni(OH) <sub>2</sub> @PANI-1 (3.2 mol%); NaBH <sub>4</sub> (10 mmol); H <sub>2</sub> O; reflux	1.5 h	85%	18
A9	Cu-BTC@Fe <sub>3</sub> O <sub>4</sub> (15 mg); NaBH <sub>4</sub> (4 mmol); CH <sub>3</sub> CH <sub>2</sub> OH : H <sub>2</sub> O (3 : 1); 45 °C	3 h	99%	19
A10	IT-MHAP-Ag (60 mg); NaBH <sub>4</sub> (5 mmol); H <sub>2</sub> O; reflux	25 min	98%	20
A11	PSeCN/Ag (20 mg); NaBH <sub>4</sub> (5 mmol); H <sub>2</sub> O; 75 °C	25 min	99%	21
A12	CoOCN (20 mg); NH <sub>2</sub> NH <sub>2</sub> ·H <sub>2</sub> O (2 mmol); H <sub>2</sub> O; 100 °C	5 h	84%	22
A13	Fe <sub>3</sub> O <sub>4</sub> @SiO <sub>2</sub> @KIT-6@2-ATP@Cu <sup>I</sup> (20 mg); NaBH <sub>4</sub> (5 mmol); H <sub>2</sub> O; r.t.	60 min	89%	23
A14	[C <sub>4</sub> (DABCO) <sub>2</sub> ] NiCl <sub>4</sub> (80 mg); NaBH <sub>4</sub> (3.5 mmol); H <sub>2</sub> O; 70 °C	1 min	98%	24
A15	Ru- <i>N,P</i> -CBM (0.02 mol% of Ru); NaBH <sub>4</sub> (5 mmol); CH <sub>3</sub> CH <sub>2</sub> OH : H <sub>2</sub> O (1 : 1); r.t.	60 min	98%	25
A16	MBC-PVIm/Pd (30 mg); NaBH <sub>4</sub> (3 mmol); H <sub>2</sub> O; 50 °C	30 min	99%	26
A17	SiO <sub>2</sub> /Fe <sub>3</sub> O <sub>4</sub> -SiO <sub>2</sub> -NH <sub>2</sub> /Cu-Ag (5 mg); NaBH <sub>4</sub> (2 mmol); H <sub>2</sub> O; 70 °C	5 min	83%	27
A18	rGO@Fe <sub>3</sub> O <sub>4</sub> /ZrCp <sub>2</sub> Cl <sub>x</sub> (x = 0, 1, 2) (20 mg); NH <sub>2</sub> NH <sub>2</sub> ·H <sub>2</sub> O (2 mmol); CH <sub>3</sub> CH <sub>2</sub> OH; reflux	10 min	98%	28
A19	Ag@VP/CTS (30 mg); NH <sub>2</sub> NH <sub>2</sub> ·H <sub>2</sub> O (5 mmol); CH <sub>3</sub> CH <sub>2</sub> OH; 70 °C	5 min	95%	29
A20	Se <sup>0</sup> (20 mol%); NaBH <sub>4</sub> (4 mmol); NaOH (1 mmol); H <sub>2</sub> O; 100 °C	3 h	88%	30
A21	CuFe <sub>2</sub> O <sub>4</sub> @SiO <sub>2</sub> @PTMS@Tu@Ni <sup>II</sup> (20 mg); NaBH <sub>4</sub> (2 mmol); H <sub>2</sub> O; 65 °C	5 min	96%	31
A22	Pd@CS-CD-MGQDs (6 mol%); H <sub>2</sub> (1 bar); deionized H <sub>2</sub> O; 50 °C	1 h	97%	32
A23	MoS <sub>2</sub> -rGO (10 mg); NH <sub>2</sub> NH <sub>2</sub> ·H <sub>2</sub> O (1.5 mmol); H <sub>2</sub> O; 100 °C	2 h	82%	33
A24	Ni <sub>2</sub> P-AC (30 mg); NH <sub>2</sub> NH <sub>2</sub> ·H <sub>2</sub> O (0.5 mL); heptane; 70 °C	2 h	93%	34

Part B				
Entry	Reaction conditions	Time	Yield	Ref.
B1	Fe <sub>3</sub> O <sub>4</sub> /f-MWCNT-CS-Glu/Ni <sup>II</sup> (5 mg); NaBH <sub>4</sub> (2 mmol); Ac <sub>2</sub> O (1 mmol); H <sub>2</sub> O; 60 °C	5 min	98%	<sup>a</sup>
B2	Fe <sub>3</sub> O <sub>4</sub> @SiO <sub>2</sub> @KCC-1@MPTMS@Cu <sup>II</sup> (10 mg); NaBH <sub>4</sub> (2 mmol); Ac <sub>2</sub> O (1 mmol); H <sub>2</sub> O; 60 °C	7 min	95%	12b
B3	(7 wt%) Pd/C (30 mg); NaBH <sub>4</sub> (2 mmol); Ac <sub>2</sub> O (1 mmol); H <sub>2</sub> O; reflux	8 min	88%	12c
B4	Cu(Hdmg) <sub>2</sub> (10 mol%); NaBH <sub>4</sub> (3 mmol); EtOAc; 60 °C	170 min	97%	12f
B5	CuFe <sub>2</sub> O <sub>4</sub> (48 mg); NaBH <sub>4</sub> (2 mmol); Ac <sub>2</sub> O (1 mmol); H <sub>2</sub> O; reflux	11 min	97%	12i
B6	Ni <sub>2</sub> B@Cu <sub>2</sub> O (54 mg); NaBH <sub>4</sub> (2.5 mmol); Ac <sub>2</sub> O (1 mmol); wet-solvent-free grinding; 40 °C	2 min	97%	12k
B7	Ni <sub>2</sub> B@CuCl <sub>2</sub> (52 mg); NaBH <sub>4</sub> (2.5 mmol); Ac <sub>2</sub> O (1 mmol); wet-solvent-free grinding; 40 °C	3 min	97%	12k
B8	[C <sub>4</sub> (DABCO) <sub>2</sub> ] NiCl <sub>4</sub> (80 mg); NaBH <sub>4</sub> (3.5 mmol); H <sub>2</sub> O; Ac <sub>2</sub> O (1 mmol); 70 °C	2 min	98%	24
B9	rGO@Fe <sub>3</sub> O <sub>4</sub> /ZrCp <sub>2</sub> Cl <sub>x</sub> (x = 0, 1, 2) (20 mg); NH <sub>2</sub> NH <sub>2</sub> ·H <sub>2</sub> O (2 mmol); Ac <sub>2</sub> O (2 mmol); CH <sub>3</sub> CH <sub>2</sub> OH; reflux	15 min	97%	28
B9	CuFe <sub>2</sub> O <sub>4</sub> @SiO <sub>2</sub> @PTMS@Tu@Ni <sup>II</sup> (20 mg); NaBH <sub>4</sub> (2 mmol); Ac <sub>2</sub> O (1 mmol); H <sub>2</sub> O; 65 °C	7 min	94%	31
B10	(2 wt%) Pd/(5 wt%) Sn-Al <sub>2</sub> O <sub>3</sub> (50 mg); H <sub>2</sub> atmosphere; Ac <sub>2</sub> O (1 mmol); H <sub>2</sub> O; r.t.	3 h	98%	35

<sup>a</sup> Present work.

## Data availability

Data will be made available on request.

## Author contributions

Hossein Mousavi: conceptualization; methodology; software; validation; formal analysis; investigation; resources; data

curation; writing – original draft; writing – review & editing; visualization; supervision; project administration. Behzad Zeynizadeh: conceptualization; methodology; validation; resources; data curation; supervision; project administration; funding acquisition. Morteza Hasanpour Galehban: conceptualization; methodology; validation; formal analysis; investigation; resources; data curation.



## Conflicts of interest

The authors declare that they have no known competing financial interests or personal relationships that could have appeared to influence the work reported in this paper.

## Acknowledgements

The authors gratefully appreciate the financial support of this work by the Research Council of Urmia University.

## References

- (a) D.-S. Zhang, Y. Liu, X. Ren, F. Geng, Y.-Z. Zhang, Y. Baikeli, M. Yang, Z. Liu, Y. Wang, X. Zhang and L. Geng, *Colloids Interface Sci. Commun.*, 2023, **56**, 100730; (b) M. Shahid, Z. H. Farooqi, R. Begum, M. Arif, W. Wu and A. Irfan, *Crit. Rev. Anal. Chem.*, 2020, **50**, 513–537; (c) P. Kovacic and R. Somanathan, *J. Appl. Toxicol.*, 2014, **34**, 810–824; (d) S. Sun, Z. Zhang, S. Li, J. Le, H. Qian, X. Yin, Y. Liu, W. Yang and Y. Chen, *J. Mater. Sci.*, 2023, **58**, 5587–5598; (e) W. Zhao, T. Wang, B. Wang, R. Wang, Y. Xia, M. Liu and L. Tian, *Colloids Surf. A: Physicochem. Eng. Asp.*, 2023, **658**, 130677; (f) L. Zhang, X. Deng, M. Hu, Y. Zhu, Z. Zhu, J. Wang, Z. Yao and H. Zhang, *Colloids Surf. A: Physicochem. Eng. Asp.*, 2023, **672**, 131735; (g) T. Huang, G. Sun, L. Zhao, N. Zhang, R. Zhong and Y. Peng, *Int. J. Mol. Sci.*, 2021, **22**, 8557; (h) S. Kazemi Movahed, P. Jafari and S. Mallakpour, *J. Environ. Eng.*, 2023, **11**, 110426; (i) S. Aghajani, M. Mohammadikish and M. Khalaji-Verjani, *Langmuir*, 2023, **39**, 8484–8493; (j) S. Nooriyan, A. Bezaatpour, A. Nuri, M. Amiri and S. Nouhi, *Catal. Commun.*, 2023, **178**, 106671; (k) S. Zhang, Q. Liu, L. Zhong, J. Jiang, X. Luo, X. Hu, Q. Liu and Y. Lu, *J. Environ. Sci.*, 2024, **138**, 458–469; (l) N. Y. Baran, M. Çalışkan, A. Özpala and T. Baran, *Int. J. Biol. Macromol.*, 2024, **262**, 130134; (m) C. C. Naik, D. P. Kamat and S. K. Gaonkar, *Int. J. Biol. Macromol.*, 2024, **286**, 131752; (n) A. Khalil, A. Khan, T. Kamal, A. A. P. Khan, S. B. Khan, M. T. S. Chani, K. A. Alzahrani and N. Ali, *Int. J. Biol. Macromol.*, 2024, **262**, 129986; (o) N. Y. Baran, *J. Organomet. Chem.*, 2024, **1008**, 123047.
- (a) M. C. Manjula, S. Manjunatha, K. L. Nagashree, M. Shivanna, M. P. Rao, N. Nanda and P. Ramachandra, *ChemistrySelect*, 2023, **8**, e202300936; (b) S. Sghajani and M. Mohammadikish, *Langmuir*, 2022, **38**, 8686–8695; (c) J. Song, Z.-F. Huang, L. Pan, K. Li, X. Zhang, L. Wang and J.-J. Zou, *Appl. Catal., B*, 2018, **227**, 386–408; (d) S. Kumar and S. K. Maurya, *J. Org. Chem.*, 2023, **88**, 8690–8702; (e) X. Li, J. An, Z. Gao, C. Xu, Y. Cheng, S. Li, L. Li and B. Tang, *Chem. Sci.*, 2023, **14**, 3554–3561; (f) S. Karimi, M. Gholinejad, R. Khezri, J. M. Sansano, C. Nájera and M. Yus, *RSC Adv.*, 2023, **13**, 8101–8113; (g) H. Jiang, G. Yuan, Z. Cui, Z. Zhao, Z. Dong, J. Zhang, Y. Cong and X. Li, *Ind. Eng. Chem. Res.*, 2023, **62**, 13355–13367; (h) H. Yu, J. Liu, Q. Wan, G. Zhao, E. Gao, J. Wang, B. Xu, G. Zhao and X. Fan, *Mol. Catal.*, 2023, **540**, 113045; (i) Z. Ma, J. Chen, M. Chen, L. Dong, W. Mao, Y. Long and J. Ma, *Mol. Catal.*, 2023, **547**, 113372; (j) S. Taheri, M. M. Heravi and A. Saljooqi, *Sci. Rep.*, 2023, **13**, 17566; (k) Y. Wei, S. Wang, Y. Zhang, M. Li, J. Hu, Y. Liu, J. Li, L. Yu, R. Huang and D. Deng, *ACS Catal.*, 2023, **13**, 15824–15832; (l) Y. Wang, X.-Y. Ye and G.-Z. Han, *Colloids Surf. A: Physicochem. Eng. Asp.*, 2024, **682**, 132869; (m) J. Wu, W. Lang, H. Li, K. Du, J. Deng, S. Zhao, W. Zhang, Z. Peng and Z. Liu, *ACS Sustainable Chem. Eng.*, 2023, **11**, 14960–14968; (n) J. Ma, X. Mao, C. Hu, X. Wang, W. Gong, D. Liu, R. Long, A. Du, H. Zhao and Y. Xiong, *J. Am. Chem. Soc.*, 2024, **146**, 970–978; (o) A. Singh, O. Singh, A. Maji, S. Singh, N. Singh, P. K. Maji and K. Ghosh, *Mol. Catal.*, 2024, **555**, 113835; (p) W. Gao, Y. Gao, B. Liu, J. kang, Z. Zhang, M. Zhang and Y. Zou, *RSC Adv.*, 2024, **14**, 5055–5060; (q) Z. Kefayati, M. Malmir and M. M. Heravi, *Res. Chem. Intermed.*, 2024, **50**, 127–146.
- K. Pierzchała, J. Pięta, M. Pięta, M. Rola, J. Zielonka, A. Sikora, A. Marcinek and R. Michalski, *Chem. Res. Toxicol.*, 2023, **36**, 1398–1408.
- M. E. González-Trujano, G. Urbie-Figueroa, S. Hidalgo-Figueroa, A. L. Martínez, M. Déciga-Campos and G. Navarrete-Vazquez, *Biomed. Pharmacother.*, 2018, **101**, 553–562.
- M. M. Alam, N. I. Alsenani, A. A. Abdelhamid, A. Ahmad, O. A. Baothman, S. A. Hosawi, H. Altayeb, M. S. Nadeem, V. Ahmad, S. Nazreen and A. A. Elhenawy, *Arch. Pharm.*, 2024, **357**, 2300340.
- (a) J. B. Zimmerman, P. T. Anastas, H. C. Erythropel and W. Leitner, *Science*, 2020, **367**, 397–400; (b) H. C. Erythropel, J. B. Zimmerman, T. M. de Winter, L. Petitjean, F. Melnikov, C. H. Lam, A. W. Lounsbury, K. E. Mellor, N. Z. Janković, Q. Tu, L. N. Pincus, M. M. Falinski, W. Shi, P. Coish, D. L. Plata and P. T. Anastas, *Green Chem.*, 2018, **20**, 1929–1961; (c) T. Keijer, V. Bakker and J. C. Slootweg, *Nat. Chem.*, 2019, **11**, 190–195; (d) P. Anastas and N. Eghbali, *Chem. Soc. Rev.*, 2010, **39**, 301–312; (e) M. Rimaz, Z. Jalalian, H. Mousavi and R. H. Prager, *Tetrahedron Lett.*, 2016, **57**, 105–109; (f) M. Rimaz, H. Mousavi, P. Keshavarz and B. Khalili, *Curr. Chem. Lett.*, 2015, **4**, 159–168; (g) M. Rimaz, H. Mousavi, M. Behnam and B. Khalili, *Curr. Chem. Lett.*, 2016, **5**, 145–154; (h) M. Rimaz, H. Mousavi, B. Khalili and F. Aali, *J. Chin. Chem. Soc.*, 2018, **65**, 1389–1397; (i) M. Rimaz, H. Mousavi, B. Khalili and L. Sarvari, *J. Iran. Chem. Soc.*, 2019, **16**, 1687–1701; (j) N. Khaleghi, M. Esmkhani, M. Noori, N. Dasyafteh, M. Khalili Ghomi, M. Mahdavi, M. H. Sayahi and S. Javanshir, *Nanoscale Adv.*, 2024, **6**, 2337–2349.
- (a) H. Mousavi, *Int. J. Biol. Macromol.*, 2021, **186**, 1003–1166; (b) Á. Molnár, *Coord. Chem. Rev.*, 2019, **388**, 126–171; (c) A. Dhakshinamoorthy, M. Jacob, N. S. Vignesh and P. Varalakshmi, *Int. J. Biol. Macromol.*, 2021, **167**, 807–833; (d) A. Brik, M. El Kadiri, T. El Assimi, P. Dambrosio, R. Beniazza, G. Gouhier, A. El Kadib and M. Lahcini, *Mol. Catal.*, 2023, **548**, 113422; (e) P. Kaur, K. K. Gurjar, T. Arora, D. Bharti, M. Kaur, V. Kumar, J. Parkash and



- R. Kumar, *Mol. Catal.*, 2023, **550**, 113582; (f) M. Çalişkan and T. Baran, *J. Organomet. Chem.*, 2022, **963**, 122284; (g) R. Beiranvand and M. G. Dekamin, *Heliyon*, 2023, **9**, e16315; (h) M. Zeyadi and Y. Q. Almulaiky, *Heliyon*, 2023, **9**, e21169; (i) F. Zhao, H. Yang, Z. Gao, H. Liu, P. Wu, B. Li, H. Yu and J. Shao, *Heliyon*, 2024, **10**, e23563; (j) P. L. Deena, S. J. Selvaraj and K. J. Thomas, *Curr. Chem. Lett.*, 2024, **13**, 359–366.
- 8 (a) D. S. Su, S. Perathoner and G. Centi, *Chem. Rev.*, 2013, **113**, 5782–5816; (b) M. E. Khan, *Nanoscale Adv.*, 2021, **3**, 1887–1900; (c) J. Zhu, A. Holmen and D. Chen, *ChemCatChem*, 2013, **5**, 378–401.
- 9 (a) B. Majumdar, S. Mandani, T. Bhattacharya, D. Sarma and T. K. Sarma, *J. Org. Chem.*, 2017, **82**, 2097–2106; (b) H. Saeidiroshan and L. Moradi, *J. Organomet. Chem.*, 2019, **893**, 1–10; (c) M. Gholinejad, H. Esmailoghli and F. Khosravi, *J. Organomet. Chem.*, 2022, **963**, 122295; (d) S. R. Mathapati, R. C. Alange, C. B. S. Mol, S. S. Bhande and A. H. Jadhav, *Res. Chem. Intermed.*, 2022, **48**, 4901–4928; (e) N. Karimi Hezarcheshmeh and J. Azizian, *Mol. Divers.*, 2022, **26**, 2011–2024; (f) K. A. Wilson, L. A. Picinich and A. R. Siamaki, *RSC Adv.*, 2023, **13**, 7818–7827; (g) D. Geedkar, A. Kumar and P. Sharma, *J. Heterocycl. Chem.*, 2020, **57**, 4331–4347; (h) M. Abdoli, N. Nami and Z. Hossaini, *J. Heterocycl. Chem.*, 2021, **58**, 523–533; (i) L. Hasani, E. Ezzatzadeh and Z. Hossaini, *J. Heterocycl. Chem.*, 2023, **60**, 2023–2035; (j) E. Ezzatzadeh, M. Mohammadi, M. Ghambarian and Z. Hossaini, *Appl. Organomet. Chem.*, 2023, **37**, e7252; (k) E. Ezzatzadeh, M. Mohammadi, Z. Hossaini and S. Khandan, *ChemistrySelect*, 2023, **8**, e202302491; (l) E. Ezzatzadeh, S. Soleimani-Amiri, Z. Hossaini and K. Khandan Barani, *Front. Chem.*, 2022, **10**, 1001707; (m) E. Ezzatzadeh, Z. Hossaini, S. Majedi and F. H. S. Hussain, *Polycycl. Aromat. Comp.*, 2023, **43**, 4707–4728; (n) M. Jahandar Lashaki, R. Hajinasiri, Z. Hossaini and N. Nami, *Polycycl. Aromat. Comp.*, 2023, **43**, 6088–6106; (o) M. M. Kadhim, N. Tabarsaei, M. Ghorchibeigi and A. Sadeghi Meresht, *Polycycl. Aromat. Comp.*, 2023, **43**, 5785–5806; (p) S. Soleimani-Amiri, M. Mohammadi, N. Faal Hamedani and B. Dehbandi, *Polycyclic Aromat. Compd.*, 2023, **43**, 6046–6075; (q) Z. Azizi, M. Ghazvini, S. Afrashteh and Z. Hossaini, *Polycycl. Aromat. Comp.*, 2024, **44**, 2508–2534; (r) A. Moazeni Bistgani, L. Moradi and A. Dehghani, *Catal. Commun.*, 2023, **182**, 106755; (s) A. R. Hajipour and Z. Khorasani, *Catal. Commun.*, 2016, **77**, 1–4; (t) D. Zeng, F. Wang, M. Bian, Y. Yang, W. Deng and R. Qiu, *J. Organomet. Chem.*, 2024, **1004**, 122943; (u) M. Lashanizadegan, F. Kamali, M. Ghiasi and H. Mirzazadeh, *J. Mol. Struct.*, 2024, **1295**, 136606; (v) L. Hasani, E. Ezzatzadeh and Z. Hossaini, *Mol. Divers.*, 2024, DOI: [10.1007/s11030-023-10803-7](https://doi.org/10.1007/s11030-023-10803-7), in press.
- 10 (a) C. Capello, U. Fischer and K. Hungerbühler, *Green Chem.*, 2007, **9**, 927–934; (b) D. Prat, J. Hayler and A. Wells, *Green Chem.*, 2014, **16**, 4546–4551; (c) V. Hessel, N. N. Tran, M. R. Asrami, Q. D. Tran, N. V. C. Long, M. Escibà-Gelonch, J. O. Tejada, S. Linke and K. Sunmacher, *Green Chem.*, 2022, **24**, 410–437; (d) C. J. Clarke, W.-C. Tu, O. Levers, A. Bröhl and J. P. Hallett, *Chem. Rev.*, 2018, **118**, 747–800; (e) F. P. Byrne, S. Jin, G. Paggiola, T. H. M. Petchey, J. H. Clarck, T. J. Farmer, A. J. Hunt, C. R. McElory and J. Sherwood, *Sustainable Chem. Processes*, 2016, **4**, 7; (f) H. Mousavi, B. Zeynizadeh and M. Rimaz, *Bioorg. Chem.*, 2023, **135**, 106390; (g) B. Zeynizadeh, H. Mousavi and F. Mohammad Aminzadeh, *J. Mol. Struct.*, 2022, **1255**, 131926; (h) R. N. Butler and A. C. Coyne, *Chem. Rev.*, 2010, **110**, 6302–6337; (i) A. Chanda and V. V. Fokin, *Chem. Rev.*, 2009, **109**, 725–748; (j) M.-O. Simon and C.-J. Li, *Chem. Soc. Rev.*, 2012, **41**, 1415–1427; (k) M. Rimaz, J. Khalafy, H. Mousavi, S. Bohlooli and B. Khalili, *J. Heterocycl. Chem.*, 2017, **54**, 3174–3186; (l) M. Rimaz, J. Khalafy and H. Mousavi, *Res. Chem. Intermed.*, 2016, **42**, 8185–8200; (m) Y. Jain, P. Gupta, P. Yadav and M. Kumari, *ACS Omega*, 2019, **4**, 3582–3592; (n) Y. Jain, M. Kumari and R. Gupta, *Tetrahedron Lett.*, 2019, **60**, 1215–1220.
- 11 M. Hasanpour Galehban, B. Zeynizadeh and H. Mousavi, *RSC Adv.*, 2022, **12**, 16454–16478.
- 12 (a) M. Hasanpour Galehban, B. Zeynizadeh and H. Mousavi, *J. Mol. Struct.*, 2023, **1271**, 134017; (b) M. Hasanpour Galehban, B. Zeynizadeh and H. Mousavi, *RSC Adv.*, 2022, **12**, 11164–11189; (c) B. Zeynizadeh, F. Mohammad Aminzadeh and H. Mousavi, *Res. Chem. Intermed.*, 2021, **47**, 3289–3312; (d) R. Bakhshi, B. Zeynizadeh and H. Mousavi, *J. Chin. Chem. Soc.*, 2020, **67**, 623–637; (e) B. Zeynizadeh, H. Mousavi and F. Sepehraddin, *Res. Chem. Intermed.*, 2020, **46**, 3361–3382; (f) B. Zeynizadeh, H. Mousavi and S. Zarrin, *J. Chin. Chem. Soc.*, 2019, **66**, 928–933; (g) B. Zeynizadeh, F. Sepehraddin and H. Mousavi, *Ind. Eng. Chem. Res.*, 2019, **58**, 16379–16388; (h) B. Zeynizadeh, F. Mohammad Aminzadeh and H. Mousavi, *Res. Chem. Intermed.*, 2019, **45**, 3329–3357; (i) B. Zeynizadeh, F. Mohammad Aminzadeh and H. Mousavi, *Green Process. Synth.*, 2019, **8**, 742–755; (j) H. Mousavi, B. Zeynizadeh, R. Younesi and M. Esmati, *Aust. J. Chem.*, 2018, **71**, 595–609; (k) B. Zeynizadeh, R. Younesi and H. Mousavi, *Res. Chem. Intermed.*, 2018, **44**, 7331–7352.
- 13 (a) P. Patinl, Q. Zheng, K. Kurpiewsk and A. Dömling, *Nat. Commun.*, 2023, **14**, 5807; (b) A. Darvishi, H. Bakhshi and A. Heydari, *RSC Adv.*, 2022, **12**, 16535–16543; (c) E. Valeur and M. Bradley, *Chem. Soc. Rev.*, 2009, **38**, 606–631; (d) V. R. Pattabiraman and J. W. Bode, *Nature*, 2011, **480**, 471–479; (e) S. Kumari, A. V. Carmona, A. K. Tiwari and P. C. Trippier, *J. Med. Chem.*, 2020, **63**, 12290–12358; (f) S. S. R. Gupta, A. V. Nakhate, G. P. Deshmukh, S. Periasamy, P. S. Samudrala, S. K. Bhargava and M. L. Kantam, *ChemistrySelect*, 2018, **3**, 8436–8443; (g) M. Lubberink, W. Finnigan and S. L. Flitsch, *Green Chem.*, 2023, **25**, 2958–2970; (h) Y. Ge, W. Huang, S. Ahrens, A. Spannenberg, R. Jackstell and M. Beller, *Nat. Synth.*, 2024, **3**, 202–213; (i) Q. Yan, Q.-J. Yuan, A. Shatskiy, G. R. Alvey, E. V. Stepanova, J.-Q. Liu, M. D. Kärkäs and X.-S. Wang, *Org. Lett.*, 2024, **26**, 3380–3385.





- 14 F. Piazzolla and A. Temperini, *Tetrahedron Lett.*, 2018, **59**, 2615–2621.
- 15 (a) B. H. Rostein, S. Zaretsky, V. Rai and A. K. Yudin, *Chem. Rev.*, 2014, **114**, 8323–8359; (b) A. Dömling, W. Wang and K. Wang, *Chem. Rev.*, 2012, **112**, 3083–3135; (c) F. Sutanto, S. Shaabani, C. G. Neochoritis, T. Zarganes-Tzitzikas, P. Patil, E. Ghonchepour and A. Dömling, *Sci. Adv.*, 2021, **7**, eabd9307; (d) D. Hurtado-Rodríguez, A. Salinas-Torres, H. Rojas, D. Becerra and J.-C. Castillo, *RSC Adv.*, 2022, **12**, 35158–35176; (e) M. Mazloun Farsi Baf, B. Akhlaghinia, Z. Zarei and S. S. E. Ghodsinia, *ChemistrySelect*, 2020, **5**, 15195–15208; (f) M. Rimaz, B. Khalili, G. Khatyal, H. Mousavi and F. Aali, *Aust. J. Chem.*, 2017, **70**, 1274–1284; (g) M. Rimaz, H. Mousavi, L. Nikpey and B. Khalili, *Res. Chem. Intermed.*, 2017, **43**, 3925–3937; (h) M. Rimaz, H. Mousavi, M. Behnam, L. Sarvari and B. Khalili, *Curr. Chem. Lett.*, 2017, **6**, 55–68; (i) D. Zeleke and T. Damena, *Results Chem.*, 2024, **7**, 101283; (j) N. Yaghmaeiyan, M. Mirzaei and A. Bamoniri, *Results Chem.*, 2023, **5**, 100696; (k) S. Handique and P. Sharma, *Results Chem.*, 2023, **5**, 100781; (l) S. S. Bhalodiya, M. P. Parmar, D. B. Upadhyay, C. D. Patel, D. P. Vala, D. Rajani and H. M. Patel, *Results Chem.*, 2024, **7**, 101304; (m) M. Rimaz and H. Mousavi, *Turk. J. Chem.*, 2013, **37**, 252–261; (n) J. Aboonajmi, M. Mohammadi, F. Panahi, M. Aberi and H. Sharghi, *RSC Adv.*, 2023, **13**, 24789–24794; (o) A. Ahmad, S. Rao and N. S. Shetty, *RSC Adv.*, 2023, **13**, 28798–28833; (p) M. Karimi, A. Ramazani, S. Sajjadifar and S. Rezayati, *RSC Adv.*, 2023, **13**, 29121–29140; (q) F. Mohammad Aminzadeh and B. Zeynizadeh, *Nanoscale Adv.*, 2023, **5**, 4499–4520; (r) H. Mousavi, *J. Mol. Struct.*, 2022, **1251**, 131742; (s) M. Rimaz, H. Mousavi, L. Ozzar and B. Khalili, *Res. Chem. Intermed.*, 2019, **45**, 2673–2694; (t) H. Mousavi, M. Rimaz and B. Zeynizadeh, *ACS Chem. Neurosci.*, 2024, **15**, 1828–1881.
- 16 (a) Y. Zhang, B. Han, Z. Zhang, X. Zhao, W. Li, B. Li and L. Zhu, *Green Chem.*, 2023, **25**, 6253–6262; (b) Y. L. Nunes, F. L. de Menezes, I. G. de Sousa, A. L. G. Cavalcante, F. T. T. Cavalcante, K. da Silva Moreira, A. L. B. de Oliveira, G. F. Mota, J. E. da Silva Souza, I. R. de Aguiar Falcão, T. G. Rocha, R. B. R. Valério, P. B. A. Fehine, M. C. M. de Souza and J. C. S. dos Santos, *Int. J. Biol. Macromol.*, 2021, **181**, 1124–1170; (c) M. Nourmohammadi, S. Rouhani, S. Azizi, M. Maaza, T. A. M. Msagati, S. Rostamnia, M. Hatami, S. Khaksar, E. Zarenezhad, H. W. Jang and M. Shokouhimehr, *Mater. Today Commun.*, 2021, **29**, 102798.
- 17 C. Sharma, A. K. Srivastava, A. Soni, S. Kumari and R. K. Joshi, *RSC Adv.*, 2020, **10**, 32516–32521.
- 18 V. S. Sypu, M. Bhaumik, K. Raju and A. Maity, *J. Colloid Interface Sci.*, 2021, **581**, 979–989.
- 19 S. Yang, Z.-H. Zhang, Q. Chen, M.-Y. He and L. Wang, *Appl. Organomet. Chem.*, 2018, **32**, e4132.
- 20 M. Pashaei and E. Mehdipour, *Appl. Organomet. Chem.*, 2018, **32**, e4226.
- 21 M. Piri, M. M. Heravi, A. Elhampour and F. Nemati, *J. Mol. Struct.*, 2021, **1242**, 130646.
- 22 A. K. Srivastava, H. Khandaka and R. K. Joshi, *SynOpen*, 2023, **7**, 121–129.
- 23 Z. Moradi and A. Ghorbani-Choghamarani, *Sci. Rep.*, 2023, **13**, 7645.
- 24 N. Seyedi, F. Shirini and H. Tajik, *J. Mol. Struct.*, 2023, **1285**, 135547.
- 25 M. Dabiri, A. Mnachekanian Salmasi, N. Salarinejad and S. Kazemi Movahed, *J. Mol. Struct.*, 2023, **1287**, 135609.
- 26 P. Mohammadi, M. M. Heravi, L. Mohammadi and A. Saljooqi, *Sci. Rep.*, 2023, **13**, 17375.
- 27 M. Z. Sarker, M. M. Rahman, H. Minami, M. S. I. Sarker and H. Ahmad, *Colloids Surf. A: Physicochem. Eng. Asp.*, 2023, **668**, 131447.
- 28 M. Bayzidi and B. Zeynizadeh, *RSC Adv.*, 2022, **12**, 15020–15037.
- 29 R. Taheri-Ledari, S. S. Mirmohammadi, K. Valadi, A. Maleki and A. E. Shalan, *RSC Adv.*, 2020, **10**, 43670–43681.
- 30 A. Capperucci, M. Clemente, A. Cenni and D. Tanini, *ChemSusChem*, 2023, **16**, e202300086.
- 31 B. Zeynizadeh, Z. Shokri and M. Hasanpour Galehban, *Appl. Organomet. Chem.*, 2019, **33**, e4771.
- 32 M. Esmailzadeh, S. Sadjadi and Z. Salehi, *Int. J. Biol. Macromol.*, 2020, **150**, 441–448.
- 33 J. Kaushik, C. Sharma, N. K. Lamba, P. Sharma, G. S. Das, K. M. Tripathi, R. K. Joshi and S. K. Sonkar, *Langmuir*, 2023, **39**, 12865–12877.
- 34 D. Sharma, P. Choudhary, S. Kumar and V. Krishnam, *J. Colloid Interface Sci.*, 2024, **657**, 449–462.
- 35 V. Bilakanti, N. Gutta, V. K. Velisoju, M. Dumpalapally, S. Inkollu, N. Nama and V. Akula, *React. Kinet. Mech. Catal.*, 2020, **130**, 347–362.

